ELSEVIER

International Journal of Mass Spectrometry 195/196 (2000) 121–138

International Journal of Mass Spectrometry

Study of gas-phase reactivity of positive and negative even-electron ions prepared from diethylmethylphosphonate ester in an external chemical ionization source of orthogonal tandem quadrupole/ion trap instrument

V. Steiner[a], I. Daoust-Maleval[b], J.-C. Tabet[a,*]

[a]*Laboratoire de Chimie Structurale Organique et Biologique, UMR-CNRS 7613 Université Pierre et Marie Curie, 4 place jussieu, 75252 Paris Cedex 05, France*

[b]*Laboratoire Chimie Recherche Analyse, Centre d'Etudes du Bouchet, B. P. 3, 91710 Vert-le-Petit, France*

Received 3 June 1999; accepted 29 September 1999

Abstract

Gas phase reactivity of the protonated and deprotonated diethylmethylphosphonate (DEMP), prepared under positive chemical ionization (PICI) and negative chemical ionization (NICI) conditions in an external high pressure source, was investigated using a recent homemade quadrupole filter/ion trap tandem with an orthogonal ion beam transmission. Ion chemical study with regard to unimolecular dissociation is described, especially with regard to the ion stability at different injection rf levels. The selective injection of the $DEMPH^+$ and $[DEMP - H]^-$ ions seems to be a very critical step that depends upon the helium buffer gas pressure and the injection low *m/z* cutoff values (LMCO). Indeed, if the parent ion abundance rises up to 50% of total ion current at a low injection rf level (LMCO of 25 Th), as LMCO is increased extend fragmentations are favored. Such decompositions mainly involved 1–5 proton transfers leading to competitive and/or consecutive losses of ethylene and water. The ion abundance versus the injection rf level presents real energy resolved dependence. Ion/molecule reactions initiated by reactive fragments of externally prepared $DEMPH^+$ [e.g. PO^+, $P(OH)_2^+$, $H_2C{=}P(OH)_2^+$, $O{=}P(OH)_2^+$, $H_3C{-}POEt^+$, $H_3C{-}PO(OCH_3)^+$, $H_3C(OH)_2P{=}OH^+$, $H_3C{-}PO(OEt)^+$, $CH_3(OEt)HP{=}OH^+$, $CH_3(OH)(CH_2{=}CHO)P{=}OH^+$, $CH_3(OH)(OEt)P{=}OH^+$, $CH_3(OCH_3)(CH_2{=}CHO)P{=}OH^+$] have been investigated. These fragment ions, selected using a quadrupole filter, induce selective ion/molecule reactions with the DEMP molecules directly introduced into the ion trap cell. The exothermic reactions observed are (1) a proton transfer process and (2) proton-bound dimer formation, as well as stepwise addition/elimination reactions in which the first electrophilic attack at the phosphorous site of the DEMP is followed by ethylene loss. On the other hand, by selecting and injecting negative ions like alkoxide species (externally formed from aliphatic alcohols in NICI), nucleophilic attacks such as a S_N2-P pathway on DEMP can occur. However, most of the ions are generated by elimination and/or deprotonation mechanisms. Alkoxide size and alcohol nucleophilic character significantly influence the orientation of the various ion/molecule reactions. (Int J Mass Spectrom 195/196 (2000) 121–138) © 2000 Elsevier Science B.V.

Keywords: Ion trap mass spectrometer; Ion/molecule reaction

* Corresponding author.

Dedicated to Bob Squires for his many seminal contributions to mass spectrometry and ion chemistry.

PII S1387-3806(99)00237-7

1. Introduction

Since the United Nations Chemical Weapons Convention and the Paris Treaty signature, identification and detection of volatile organic compounds, such as pesticides and chemical warfare agents and their degradation products, have been a topical subject [1,2]. This necessitates the development of analytical methods for unambiguous detection and identification of organophosphorus compounds (OPC) present in trace levels from a complex matrix.

The ion trap mass spectrometer can be a useful tool for such investigations, but applications of the commercially available quadrupole ion trap instruments are restricted to low molecular weight species and to positive ion mode. In fact, efficient in situ formation of negative ions is difficult to achieve [3,4]. Moreover, trapping of the molecular and fragment ions as well as their neutral parents during long ionization and reaction times can lead to undesirable processes such as self ionization [5], and the resulting ion/molecule reactions pose difficulties in the interpretation of conventional electron ionization (EI) mass spectra. The use of an external source for producing reagent and analyte ions seems to be an attractive alternative to overcome these difficulties [6]. Creation of reagent ions in an external ion source and their injection into the ion trap can aid the study of ion/molecule processes [7]. In order to increase the specificity of ion/molecule reactions by the selection of reagent ions, different tandem hybrid instruments have already been built by coupling a conventional ion beam analyzer with an ion trap. For example, double sector analyzers such as E/B and B/E systems [8] or more complex tandem instruments such as BE–quistor–quadrupole [9] or quadrupole–ion trap–quadrupole [10] instruments were developed.

In the present work, specific ions were prepared from DEMP using positive and negative ion chemical ionization (CI). Their behavior toward collision-induced dissociation (CID) and particular nucleophilic/electrophilic reactions yielding diagnostic ion/molecule reactions was investigated. In order to attain our goal, a homemade 90° geometry quadrupole/ion trap mass spectrometer (Q/ITMS) tandem was used. It allows one to selectively study ion/molecule reactions induced by both the thermalized positive or negative ions. A similar off-axis geometry has already been used by Pedder et al. [11]. In our improved Q/ITMS, secondary ion/molecule reactions leading to artifacts are avoided by the use of both the ion deflector lenses and by the use of differential pumping between the quadrupole mass filter and the ion trap analyzer manifolds.

2. Experimental

All experiments were performed with an off-axis geometry quadrupole/ion trap tandem (Fig. 1). The instrument was composed of a Nermag R10-10 quadrupole mass filter combined with a dual electron ionization/chemical ionization (EI/CI) source and a Finnigan Mat ion trap mass spectrometer (ITMS). A quadrupolar electrostatic deflector with a perpendicular geometry links both the linear quadrupole and the ion trap mass spectrometer.

The possibility of using this homemade tandem as a simple quadrupole analyzer or as an ion trap device permits the comparison of data recorded in different analyzing modes, but this was also important for optimizing the selected ion beam before injection into the ion trap reaction cell. The electrode potentials were adjusted according to the chosen working mode: e.g. quadrupole/MS, ITMS, or tandem Q/ITMS. The EI/CI mixed source was used as an external source: the potentials applied to the ion source and to the extractor, the ion kinetic energy, and the quadrupole deflector lenses were adjusted to optimize the ion beam transmission efficiency. The experimental conditions employed for preparing positive ions were: filament 100 mA, electron energy 90 eV, $V_{source} = 16$ V and $V_{repeller} = -18$ V, source temperature 150 °C. In ammonia CI experiments, NH_3 and DEMP pressures (not corrected) were about $P_{NH3} = 2 \times 10^{-4}$ Torr (0.03 Pa) and $P_{DEMP} = 5 \times 10^{-7}$ Torr (6.7×10^{-5} Pa). This optimization step is required before each injection experiment. The externally created ions

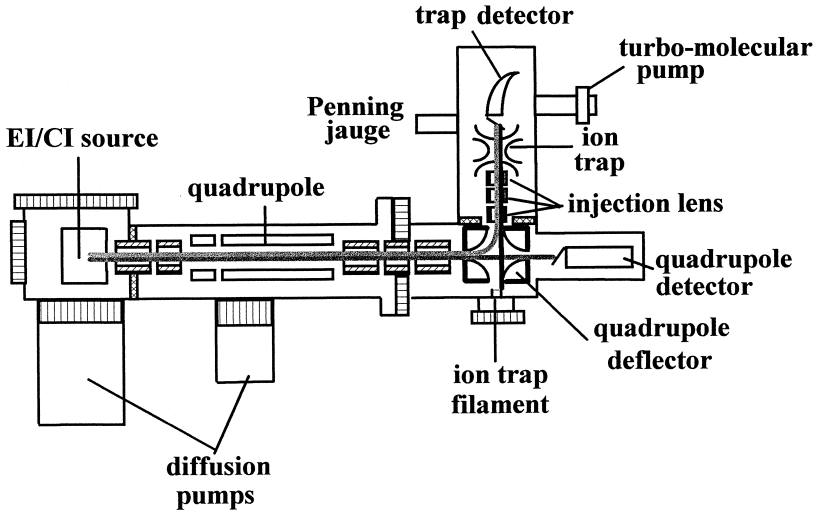

Fig. 1. Scheme of the Nermag R10-10 quadrupole mass filter combined with a modified dual EI/CI source and the Finnigan (ITMS) tandem instrument with a 90° geometry electrostatic deflector.

are then injected into the ion trap reaction cell through the quadrupolar off-line deflector lenses. However, the ion transmission efficiency has been estimated at lower than 1%, yielding a low sensitivity, so optimization of this ion injection step is essential to study the reactivity of the selected organophosphorus ions toward neutral species introduced into the ion trap reaction cell. Optimization of the injection parameters such as the injection rf amplitude level and the helium pressure (fixed at 4×10^{-4} Torr $\approx$ 0.05 Pa) also determine the trapping efficiency. Detection was achieved by using an electron multiplier (Channeltron Galileo) combined with a conversion dynode (operating voltage: $\pm$4000 V, according to the polarity of the studied ions).

The scan function employed for ion/molecule reaction studies is given in Fig. 2. After a 50 ms injection period (A), the isolation step (B) is followed by the ion/molecule reaction period (C); the produced ions were then detected by ramping the driving rf potential amplitude (scan rate: 5555 Th/s) (D) using the mass-selective instability scan [12]. The analytical scan was combined with an axial modulation [13] (1.5 V_{p-p} and $f < 550$ kHz) to improve sensitivity as well as resolution. The DEMP substrate used was given by the Centre d'Etudes du Bouchet (CEB) with a purity of 83%.

3. Results and discussion

Alkylphosphonate diester belongs to the important class of organophosphorus compounds [14]

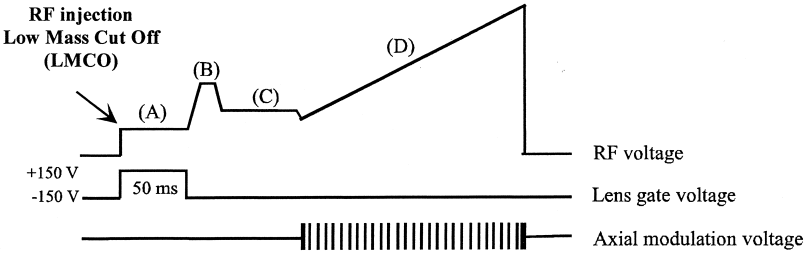

Fig. 2. Scan function employed for the ion/molecule reaction studies.

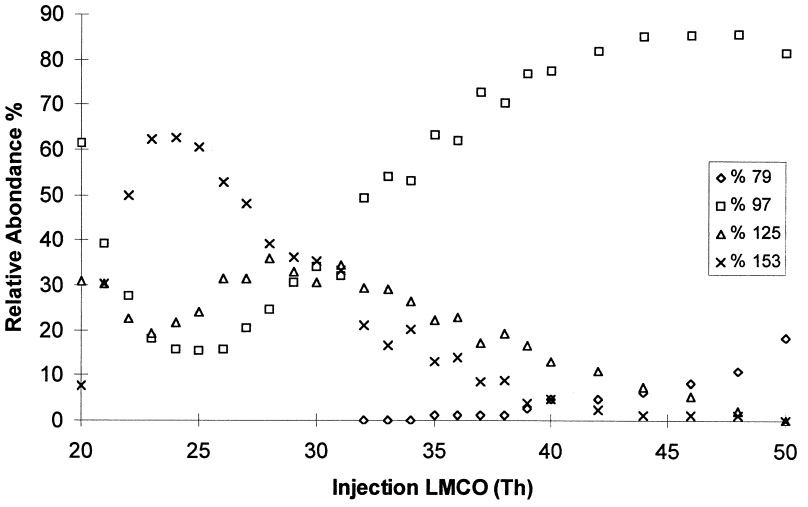

Fig. 3. Dependence of the relative abundances % of the produced ions (*m/z* 79, *m/z* 97, *m/z* 127) from the selected $DEMPH^+$ (*m/z* 153) injection upon the injection rf level potential values.

and are attractive target molecules for systematic studies of ion chemistry that might assist in terms of their identification and detection at trace levels (e.g. in environmental studies). The methylphosphonates are currently used as models under EI conditions for studying molecular ion isomerization (ester/enol as a reversible tautomeric reaction [15]). Under our conditions, in the quadrupole ion source, ionization of the diethylmethylphosphonate does not give rise to stable odd-electron $M^{+\cdot}$ molecular ions. Indeed, it decomposes readily into even-electron fragment ions (noted as FH^+); weak abundances of odd-electron fragment ions are also observed. In order to approach problems of molecular structure, fragmentations of the ionized OPC have been scrutinized in positive and negative [16,17] ion modes. Using a conventional ion trap, Mechin et al. [5] showed that under EI conditions, the odd-electron molecular ions of OPC completely decomposed and that these fragment ions gave rise to the formation of MH^+ by self-ionization processes [5]. This behavior is characteristic of DEMP, and the $DEMPH^+$ ion (*m/z* 153) is observed under EI conditions. Positive ion CI provides similar even-electron molecular species.

3.1. Optimization of $DEMPH^+$ and $[DEMP - H]^-$ injection step: influence of injection rf level on the ion stability

The injection of the protonated $DEMPH^+$ ions (*m/z* 153) was first examined and the resulting ions were analyzed by the ion trap. The quasimolecular ions were generated under ammonia PICI conditions in the external high-pressure source and were injected into the ion trap reaction cell according to various injection rf level values [called low *m/z* cutoff (LMCO) in Thomson units]. This parameter corresponds to the lower *m/z* ion that can be trapped and determines the ion position (q_z) in the stability diagram, during the injection period. The dependence of the relative abundance of the $DEMPH^+$ ions observed during the injection period versus the injection cutoff values is reported in Fig. 3.

Scrutinizing these ion dependences, it is obvious that $DEMPH^+$ is always introduced into the ion trap under favorable conditions of dissociation. Indeed, even when the linear quadrupole is used as an ion selector for selective injection of the *m/z* 153 ions, consecutive dissociations are observed and lead to the *m/z* 125, *m/z* 97, and *m/z* 79 fragment ions (Scheme

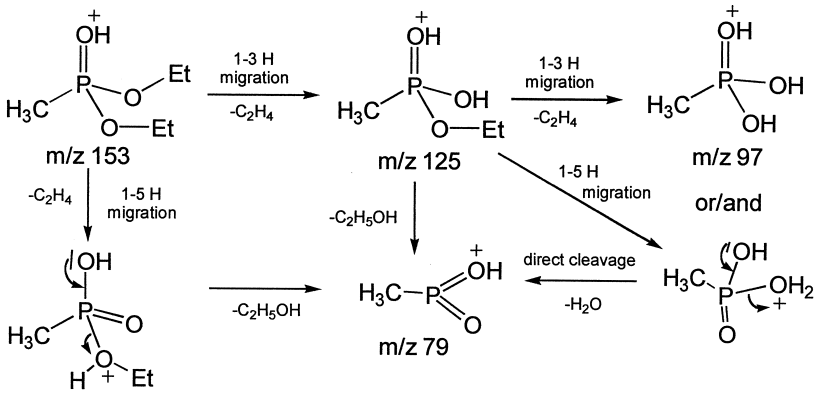

Scheme 1. Produced ions generated by consecutive decompositions of the $DEMPH^+$ ion (*m/z* 153) during its injection period.

1). Alternatively, if it is possible to detect the fragment ions through all of the studied LMCO range, then the efficient trapping of $DEMPH^+$ ions is difficult. The low LMCO range that allows the observation of the precursor *m/z* 153 ion can be explained by assuming that a minimum LMCO (which can be related to the injection q_z parameter value) is required for an efficient trapping of polyatomic ions [18]. Moreover, at high LMCO values, collisions with helium are sufficiently energetic that dissociation processes induced by collision yield a loss of the MH^+ signal intensity. The fast decline of MH^+ ion intensity as the injection q_z rises (whereas the fragment abundance increases) has also been noticed by Robb et al. [19a] and explained previously.

Another main observation is the role played by the LMCO (Fig. 3) on the orientation of the consecutive fragmentations during the ion injection step [19b]. At lower LMCO values, the first rearrangement process yielding *m/z* 125 by loss of ethylene is favored. As the rf injection level is raised, the relative abundance of both the *m/z* 153 and *m/z* 125 ions falls down. The parent ions acquire higher internal energy during the injection step due to collisions with helium atoms that lead to the $DEMPH^+$ ions dissociation, i.e. consecutive ethylene and water losses (*m/z* 97 and *m/z* 79 ions). Fig. 3 can be considered in terms of energy resolved mass spectrometry (ERMS) breakdown curves [20]. ERMS curves of organophosphonate compounds including $DEMPH^+$ ions have already been constructed by Wensing et al. [21,22] using a tandem triple quadrupole mass spectrometer. At high energy $H_2C{=}P(OH)_2^+$ (*m/z* 79) and PO^+ (*m/z* 47) ions formed due to consecutive losses of $[C_2H_5OH + H_2O]$ were detected. In the homemade Q/ITMS instrument used, the PO^+ ions were not detected even when LMCO was increased from 20–36 Th, i.e. high q_z values (0.4–0.7). This usually corresponds to an accumulation of internal energy due to an increase in kinetic energy that is consistent with the depth of the pseudo-potential well [23]. Thus, the energy deposited on the selected precursor ion during the injection step seems to be limited.

The behavior of deprotonated molecules (noted as $[DEMP - H]^-$, *m/z* 151, prepared in the external source under ammonia NICI conditions) selected through the quadrupolar filter of the tandem (Fig. 4), presents trends similar to that observed for the selected protonated molecules. Indeed, the better trapping efficiency of the injected $[DEMP - H]^-$ ions corresponds to a LMCO value of 25 Th, as observed for the $DEMPH^+$ ions. Moreover, dissociation activation takes place during the injection step and fragment ions are produced. However, by comparing the behavior of the ions in positive and negative modes, some differences can be highlighted: (1) at low LMCO values, the precursor $[DEMP - H]^-$ ion appears much more abundant (45% of the ionic current) than the $DEMPH^+$ (10% of the ionic current), as shown by the breakdown curves (Figs. 3 and 4). As the LMCO is increased, relative abundance of the species reaches 55% for both ions. However,

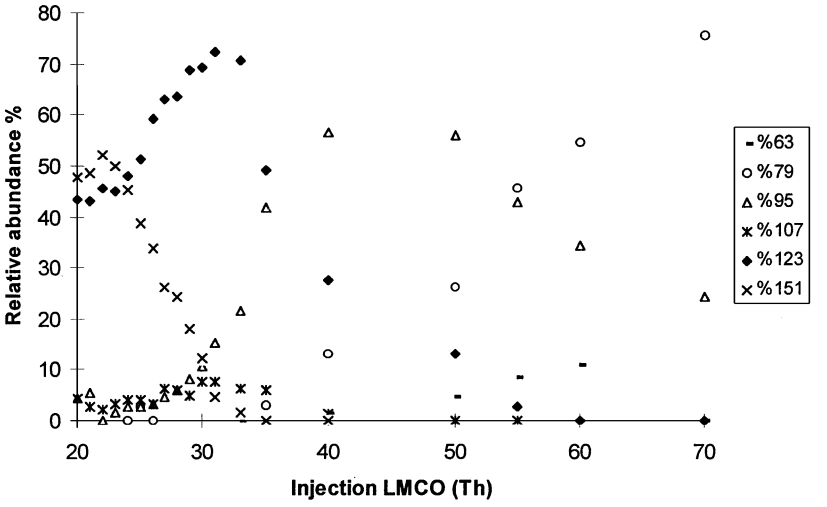

Fig. 4. Dependence of the relative abundances % of the produced ions (*m/z* 63, *m/z* 79, *m/z* 95, *m/z* 107, *m/z* 123, *m/z* 151) from selected $[DEMP - H]^-$ (*m/z* 151) injection upon the injection rf level potential values.

$[DEMP - H]^-$ ions completely disappear when the LMCO exceeds 35 Th, whereas $DEMH^+$ ions are observed for LMCO up to 50 Th. (2) In the negative mode numerous dissociative processes are observed. The major direct C_2H_4 loss ($[DEMP - H - C_2H_4]^-$ *m/z* 125 70% of the ion current at a LMCO of 30 Th) competes with the minor C_2H_4O elimination (*m/z* 107, 7% of the ionic current at a LMCO of 30 Th, Scheme 2). For a LMCO greater than 35 Th, competitive loss of C_2H_4 and C_2H_4O from the $[(DEMP - H) - C_2H_4]^-$ ions takes place (Scheme 2), leading to the formation of *m/z* 95 and *m/z* 79, respectively. (3) Consecutive loss of two C_2H_4O ions (i.e. $[(DEMP - H) - 2C_2H_4O]^-$, *m/z* 63) can also occur and similar elimination has already been observed in the positive mode from $DEMPH^+$ in triple quadrupole instrument experiments [21,24] yielding $[DEMPH - 2C_2H_4O]^+$ (*m/z* 65). Such consecutive dissociations are not detected in the tandem instrument. Instead, a weak signal corresponding to the *m/z* 79 ion is observed,

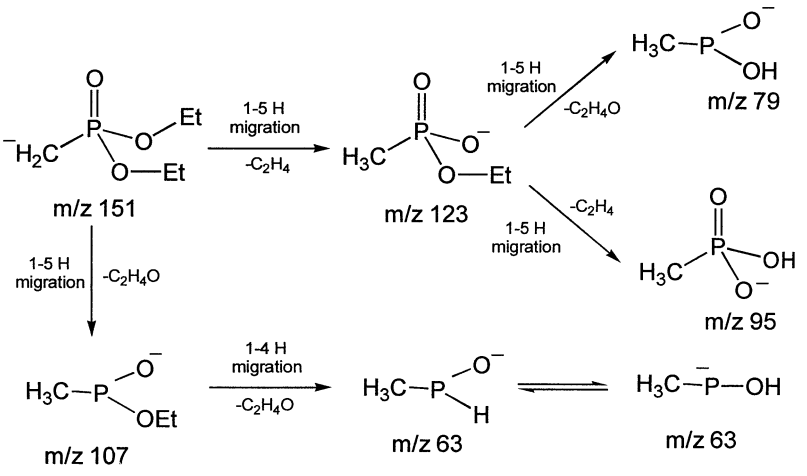

Scheme 2. Produced ions during injection of the selected $[DEMP - H]^-$ ions (*m/z* 151).

coming either from *m/z* 97 ions via consecutive water loss $[DEMPH - 2C_2H_4 - H_2O]^+$ or from direct elimination of ethanol from the fragment *m/z* 125 ions (Scheme 1).

At low LMCO values, the weak dissociation yielding consecutive C_2H_4 losses indicates that the $[DEMP - H]^-$ ions are more stable than the protonated $DEMPH^+$ molecules. This is confirmed by the shift of the ion appearance LMCO threshold of $[(DEMP - H) - 2C_2H_4]^-$ (*m/z* 95) compared to that of the LMCO threshold of the *m/z* 97 ions. In order to reach a relative intensity of 10%, the LMCO value has to be higher than 30 Th, whereas for the corresponding $[DEMPH - 2C_2H_4]^+$ (*m/z* 97) obtained from a positive even-electron ion precursor, the relative intensity is already greater than 10% at a LMCO of 20 Th. Such a stability is expected because the exothermicity of the deprotonation reaction is carried out by the lost neutral. The deprotonated molecules obtained under NICI conditions are then generally assumed to be stable in contrast with the protonated molecules that carry out exothermicity of the proton transfer reaction [25]. Furthermore, the special nature of the charged $P–O^-$ bond confers a good stability to $[DEMP - H]^-$ compared to that of the positively charged $P=OH^+$ bond in the protonated $DEMPH^+$ molecules. On the other hand, this implies that the $P=OH^+$ is more activated than the negatively charged $P–O^-$ bond.

3.2. Ion/molecule reactions between FH^+ fragment ions and DEMP molecules

FH^+ fragment ions, generated under EI conditions by the dissociation of odd-electron $DEMP^{+\cdot}$ molecular ions were selectively injected into the ion trap reaction cell to react with DEMP through a liquid sample introduction system. No attention was paid to the reactivity of the odd-electron ions ($DEMP^{+\cdot}$ or fragment ions) injection and reactivity. The tautomeric reaction observed in the $M^{+\cdot}$ ion is described in literature [15], but such a 1–3 proton transfer is not mentioned for MH^+ or FH^+ ions and will not be considered in the following discussion. Indeed, formation of a protonated enolic $CH_2=P(OC_2H_5)_2OH_2^+$ form should not be reactive toward electrophilic attachment with DEMP and will isomerize into its initial ester form prior to any bimolecular process. Ions resulting from the FH^+/DEMP reactions, generated after a reaction time of 20 ms, are summarized in Table 1. Similar experiments have already been performed in an in situ ionization conventional ion trap [5b] (not discussed here). The information obtained from reaction in the tandem can help one to better understand the processes that took place during in situ experiments. The usual $DEMPH^+$ ions (*m/z* 153) and the $[DEMP]_2H^+$ dimeric ions (*m/z* 305) were formed from ion/molecule reactions induced by all selected reagent ions (i.e. FH^+ fragment ions). The solvation reactions of the even-electron ion are always exothermic processes because charge solvation constitutes a significant potential energy stabilization through charge dilution. In certain cases $[DEMP, FH]^+$ can, however, be detected under low abundance according to two modes.

The first mode of attachment, which involves the orientation for the formation of noncovalent adduct species, depends upon the protonated MH^+ molecule or even-electron fragment FH^+ ions ability to generate long-life proton bound homogeneous or heterogeneous dimers [26] by reaction with the DEMP neutral. To observe such proton-bound dimers: (1) the components (constituted by electron lone pairs and/or unsaturation) of the dimer must have similar gas phase basicities [27]. (2) The proton affinity of both components must be as low as possible [27]. (3) The depth of the potential energy well characterizing the solvation process must be sufficiently large (e.g. from 40–100 kJ mol^{-1}) [28].

The FH^+ fragment ions such as $[(H_3C)(H_3CO)(CH_2=CHO)P=OH^+]$ (*m/z* 137), $[(H_3C)(HO)(C_2H_5O)P=OH^+]$ (*m/z* 125), $[(H_3C)(HO)(CH_2=CHO)P=OH^+]$ (*m/z* 123), $[(H_3C)(HO)_2P=OH^+]$ (*m/z* 97), $[O=P(OH)_2^+]$ (*m/z* 81), $[H_2C=P(OH)_2^+]$ (*m/z* 79), and $[P(OH)_2^+]$ (*m/z* 65) can be considered protonated forms of alkyl or dialkyl phosphonic acid. They are characterized by lower proton affinity than the corresponding diester phosphonates [29] and they can yield noncovalent heterodimers as well as proton exchange processes that can compete with other reaction pathways.

Table 1
Detected ions during the ion/molecule reaction between the FH^+ fragment ions and DEMP neutrals, using the tandem Q/ITMS after 20 ms reaction time (the ion abundances normalized at 100% of the total ionic current are reported in brackets)

Selected reagent ion FH^+ (F^+)	$[FH^+ + M]$ or $[F^+ + M]$ A^+	$[A - 28]^+$ B^+	$[B - 28]^+$ C^+	$[C - 78]^+$ D^+	$DEMPH^+$ *m/z* 153 MH^+	$DEMP_2H^+$ *m/z* 305 M_2H^+	Other ions
m/z 47 (29.6)	*m/z* 199 (0.5)	*m/z* 171 (0.7)	*m/z* 143 (11.9)		(26.6)	(9.9)	*m/z* 97 (20) *m/z* 125 (0.4)
m/z 65 (20.4)					(40.9)	(36.9)	*m/z* 97 (0.7) *m/z* 125 (0.6)
m/z 79 (31.4)		*m/z* 203 (1.2)	*m/z* 175 (7.4)	*m/z* 97 (28.7)	(24.8)	(5.6)	*m/z* 125 (0.4) *m/z* 143 (0.4)
m/z 81 (48.5)			*m/z* 177 (1)	*m/z* 99 (30.2)	(31)	(8.1)	*m/z* 125 (1)
m/z 91 (3.4)	*m/z* 243 (1.6)	*m/z* 215 (0.75)	*m/z* 187 (1.3)	*m/z* 109 (37)	(35.6)	(17.2)	*m/z* 97 (0.6) *m/z* 125 (0.6)
m/z 93 (22.2)		*m/z* 217 (0.4)	*m/z* 189 (0.4)	*m/z* 111 (5.2)	(49.7)	(20.2)	*m/z* 97 (0.6) *m/z* 125 (0.7)
m/z 97 (43.6)					(37.5)	(16.7)	*m/z* 125 (0.1) *m/z* 175 (1.6)
m/z 107 (2.9)		*m/z* 231 (0.3)	*m/z* 203 (1.9)	*m/z* 125 (1.7)	(57.6)	(22.4)	*m/z* 97 (4.7) *m/z* 175 (10.6)
m/z 109 (35.6)					(44)	(16.1)	*m/z* 97 (0.4) *m/z* 125 (0.25)
m/z 123 (23.9)					(49.6)	(25.7)	*m/z* 125 (0.5)
m/z 125 (24.6)	*m/z* 277 (1.5)				(46.5)	(27)	
m/z 137 (19.3)	*m/z* 289 (2.2)				(38.8)	(27.2)	*m/z* 125 (0.4)

The second mode of attachment implies a covalent charge solvation and may take place if the energy pathway does not have a large intrinsic barrier, which kinetically limits the efficiency of the ion/molecule reaction, hindering the formation of product ions coming from the attachment processes.

Considering the fact that the heterodimer ions observed exist within the covalent and noncovalent forms, the results reported in Table 1 allow one to classify the reactant ions according to their potential capacity to produce one form or another preferentially. However, the important reaction pathway is always the protonation and the formation of [DEMP, FH^+] and the heterodimer may be considered to be formed through a minor pathway. Furthermore, protonation may take place by proton exchange from second generation product ions as well as directly from FH^+ ions through formation of excited [DEMP, FH^+] ions.

So, three different types of FH^+ reagent ions (or nonprotonated even-electron F^+ species, as PO^+) can be described: (1) the selected *m/z* 125 and *m/z* 137 ions leading to relatively stable noncovalent heterogeneous dimers that partially decompose into the FH^+ and $DEMPH^+$ ions according to the respective basicity of the corresponding neutrals; (2) the selected *m/z* 65, *m/z* 97, *m/z* 109, and *m/z* 123 ions for which no heterogeneous dimers (very reactive towards dissociations) are detected; (3) the ions yielding preferentially covalent heterogeneous dimers (i.e. *m/z* 47, *m/z* 79, *m/z* 81, *m/z* 91, *m/z* 93, *m/z* 107), that can dissociate by loss of small neutral species, such as C_2H_4.

In the ion trap reaction cell, the selected and injected ions exothermically react with the introduced DEMP sample and the ions formed can possess significant internal energy. Collisional relaxation of internal energy by helium must be inefficient [30a] in contrast to collisions produced with the neutral sample [30b] even if present in weak partial pressure compared to the helium bath gas. Note that the internal energy relaxation of covalent adduct species must differ during collision with the DEMP neutral species because of the cross section variation due to

modification of the charge environment (steric hindrance of the DEMP approach). Thus, mainly two populations of solvated ions [FH^+, DEMP] (or [F^+, DEMP]), i.e. both the relaxed and excited species must be considered according to their respective structure (Table 1). Similar species were found in experiments with a conventional ion trap in which the FH^+ and F^+ ions [5b] were prepared.

Formation of characteristic *m/z* 97 and *m/z* 125 product ions was observed in most of the experiments. It is difficult to know whether they were formed by the decompositions of the $DEMPH^+$ ions (*m/z* 153) or by the consecutive fragmentations of covalent dimeric ions. The decompositions of MH^+ ions cannot be ruled out. Considering the fact that exothermicity of the MH^+ formation increases as the reactant *m/z* decreases, it is expected that the internal energy of the formed *m/z* 153 ions will be larger when the ions are generated by the ion/molecule reactions with smaller reagent ions. So, importance of the consecutive losses from $DEMPH^+$ ions (measured from the *m/z* 97/*m/z* 125 ratio) should be greater as the reagent ion *m/z* value decreases. Because this ratio seemed rather constant (except for the particular *m/z* 47, *m/z* 79, and *m/z* 81 reagent ions), it can be assumed that the protonated *m/z* 153 molecules are sufficiently relaxed by collision with the DEMP neutrals and thus, the exothermicity of ion/molecule reactions is dispersed. Consequently, other origins must be proposed for these *m/z* 97 and *m/z* 125 fragment ions and only the formation of such ions with an abundance greater than 1% are discussed here.

3.2.1. Proton-bound homogeneous dimers $[DEMP]_2H^+$ and noncovalent heterogeneous [FH^+, DEMP] forms

In most of the cases (Table 1), the proton-bound heterodimers should be highly unstable and should readily decompose according to higher rate constants than those of the more stable covalent dimers. Their formation can be followed by dissociation [less endothermic pathway, Eq. (1)] or they can react with a DEMP neutral yielding a more stable $[DEMP]_2H^+$ homogenous dimer by ligand F/DEMP exchange [Eq. (2)].

The dissociation orientation of the [FH^+, DEMP] heterodimer towards the competitive formation of $DEMPH^+$ rather than FH^+ [Eq. (1)] corresponds to a lower endothermic dimer dissociation because proton affinity (PA) of the DEMP neutral must be higher than any F fragment neutral. In most of the ion/molecule reactions, the total ionic current of the $DEMPH^+$ and $[DEMP]_2H^+$ ions is higher than (or close to) any product ion and even greater than the FH^+ abundances (Table 1).

Reaction of the excited [DEMP, FH^+]* heterodimeric ions towards DEMP leads to formation of proton-bound homogeneous $[DEMP]_2H^+$ dimers. This ligand exchange will be exothermically favored [Eq. (2)] because $PA_F < PA_{DEMP}$, as assumed previously. This means that the homogeneous proton-bound dimers are expected to be more stable than the heterogeneous proton bound dimers [27b]. Furthermore, it is expected that stabilizing collisions with DEMP yield more internal energy relaxation for the $[DEMP]_2H^+$ ion than for the unstable [DEMP, FH^+] heterodimer.

The fact that the noncovalent dimers are stable if the PA of both components are close permits one to explain why the [DEMP, FH^+] dimer ions (i.e. *m/z* 277 and *m/z* 289) were observed with the *m/z* 125 and *m/z* 137 monoester reagent ions, respectively. Thus, no consecutive decomposition is detected, so the corresponding [FH^+, DEMP] dimers can be considered a noncovalent system because decompositions of

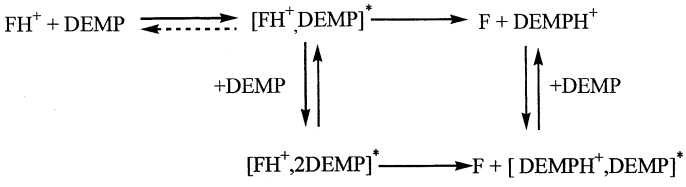

the proton bound dimer yields either $DEMPH^+$ and/or FH^+ and not fragment ions due to ethylene loss. To be characterized by such a reactivity, proton affinity of the $(H_3C)(OH)(OEt)P{=}O$ neutral (corresponding to the *m/z* 125 ion) has to be sufficiently close to that of the DEMP diester to yield the *m/z* 277 dimer (i.e. 1.5% Table 1). For the reagent ion at *m/z* 137, such behavior cannot be expected because the ion structure already known is in unprotonated form. A kind of particular isomerization must likely take place to yield observation of the exothermic proton transfer. This idea has not been developed herein, however, experiments using deuterium labeling could help to rationalize the mechanism of this reaction. We emphasize that the reactions between reagent ions prepared in the ion trap mass spectrometer and the DEMP neutrals also allow the formation of $[DEMP]_2H^+$ ions, although its abundance is closer or slightly lower than that observed from the tandem Q/ITMS experiments.

3.2.2. Observation of covalent dimers

Another class of reagent ions including $[P{=}O^+]$ *m/z* 47, $[H_2C{=}P(OH)_2^+]$ *m/z* 79, $[O{=}P(OH)_2^+]$ *m/z* 81, $[H_3C{-}P{=}OEt^+]$ *m/z* 91, $[H_3C{-}P{=}O(OCH_3)^+]$ *m/z* 93, and $[H_3C{-}P{=}O(OEt)^+]$ *m/z* 107 present a characteristic behavior toward the DEMP molecule. The reactivity of these reagent ions seems very similar. Indeed, all of these ion/molecule reactions yield: (1) mainly homogeneous proton-bound $[DEMP]_2H^+$ dimer ions by the exothermic exchange of ligand FH^+/DEMP (or $[F^+$/DEMP], Table 1) that dissociate into $DEMPH^+$ as the major ion; (2) the excited covalent $[FH^+$, DEMP] dimers, for a minor contribution that are produced by an electrophilic attack at phosphorus atom induced by the FH^+/F^+ reagent ion. These dimers promptly decompose by consecutive losses of two ethylene molecules and finally by the loss of a 78 u neutral (i.e. CH_3PO_2) as reported in Scheme 3.

In most of the reactions, a weak abundance of *m/z* 97 and *m/z* 125 product ions (generated from the covalent adduct ions) can be noticed (Table 1). However, the protonated methylphosphonate diacid *m/z* 97 is provided in a relatively significant abundance from the *m/z* 47, *m/z* 79, and *m/z* 107 reagent ions (i.e. 20%, 30%, and 5%, respectively). These ions can have a different origin; ions coming from reaction with the *m/z* 47 reagent ion can be produced from the dissociation of the adduct $[PO^+$, DEMP]. By consecutive losses of two C_2H_4 (Scheme 4) a *m/z* 143 ion is formed and can react with a second DEMP neutral via a second electrophilic attack. The final loss of 78 u (i.e. CH_3PO_2) should yield fragment ions expected at *m/z* 65 [Scheme 3(a)] nevertheless, those ions are not detected. This can be explained by considering that the *m/z* 65 ions can competitively react with DEMP molecules to produce MH^+ ions (Table 1).

For *m/z* 97 formed by the reaction of DEMP with *m/z* 107 and *m/z* 79, different pathways can be proposed: either the consecutive decompositions of their respective covalent $[DEMP, 107]^+$ and $[DEMP, 79]^+$ adduct ions (Scheme 5) or the dissociation of the ion dipole complex [Scheme 5(c)] into *m/z* 97 rather than into the complementary *m/z* 79 ion (similar to the precursor ion). The observation of *m/z* 97 from the latter ion is possible because the basicity of CH_3PO_2 is lower than that of $CH_3P(OH)_2O$. The presence, in most of the reactions, of small *m/z* 125 ions was also elucidated by fragmentation of the covalent dimer after the simple loss of one ethylene molecule; the proposed mechanism is shown in Scheme 3(c) for the *m/z* 107 reagent ions.

Looking at these results, it seems that the distribution of the kinetic energy of the ions injected using Q/ITMS tandem is broader than that found for the in situ ionization experiments [5b]. Indeed, a fraction of the injected ions relaxes kinetically by collision with helium atoms that allow production of $[DEMP]_2H^+$ adduct ions in high abundance. The remaining ions do not relax efficiently and they carry higher internal energy. It can be considered that the reactions leading to the fragmentation of $[FH, DEMP]H^+$ covalent heterodimers are necessarily endothermic via a tight transition state. A significant amount of internal energy is required to cross the bottleneck of the reaction for consecutive decomposition. Because they are present in significant abundance it can be assumed that part of these dimers are excited in the tandem.

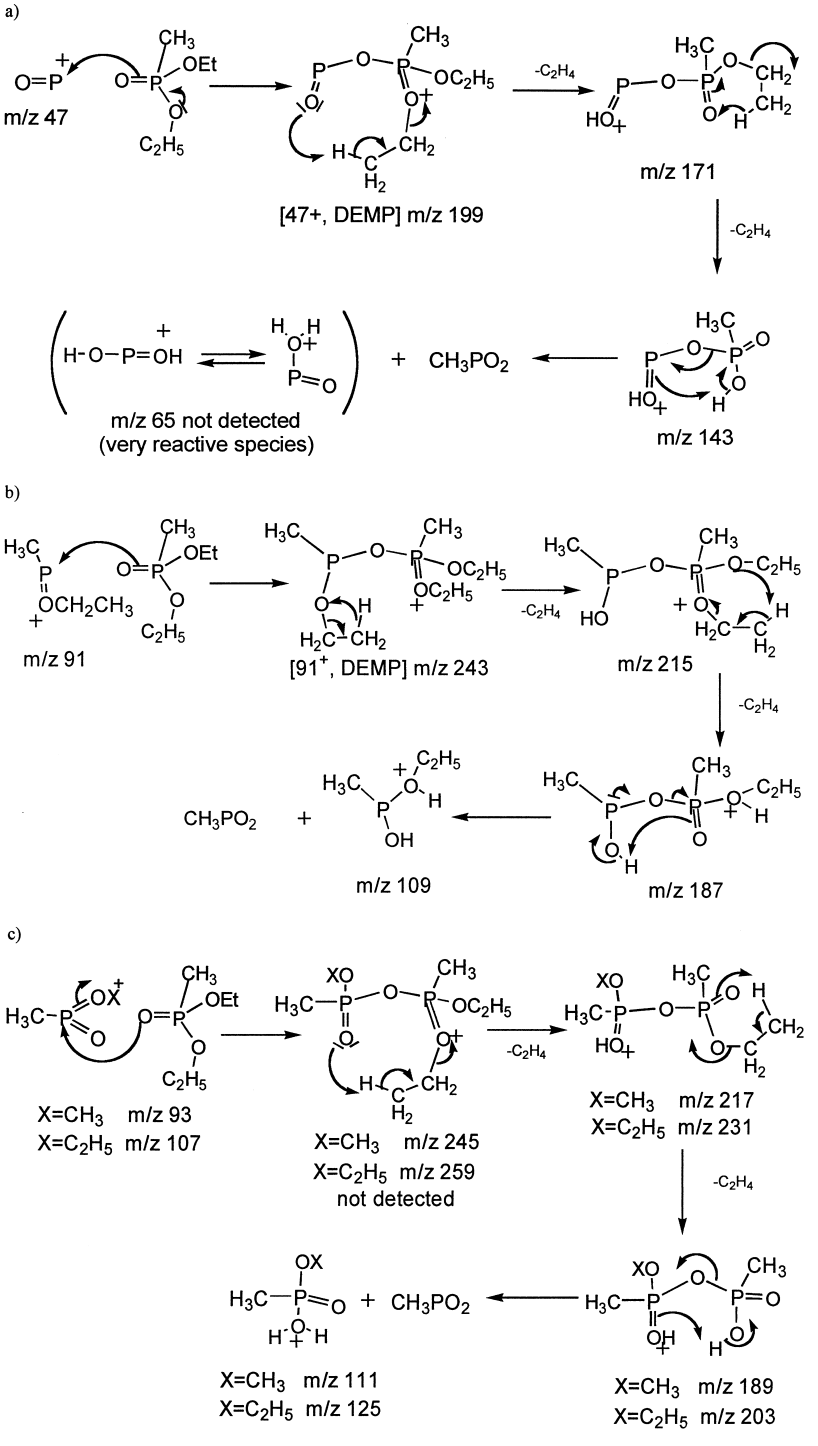

Scheme 3. Consecutive decomposition yielding losses of two ethylene molecules and a loss of a 78 u neutral by reaction of (a) *m/z* 47, (b) *m/z* 91, (c) *m/z* 93, and *m/z* 107 ions on DEMP, from the minor covalent [FH^+, DEMP] adduct ions.

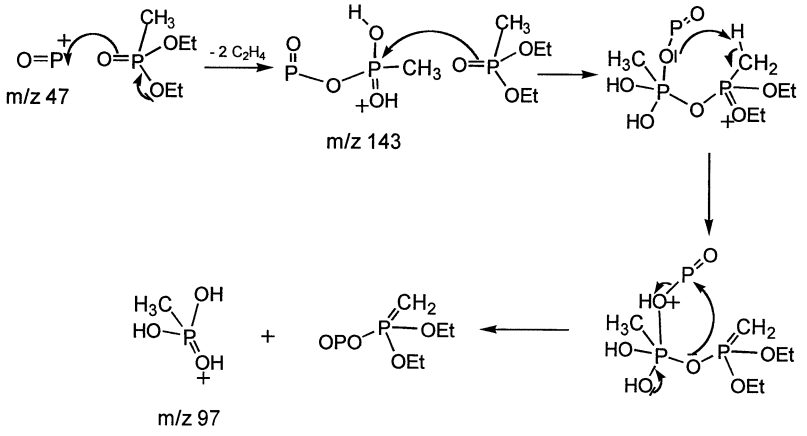

Scheme 4. Particular formation of the *m/z* 97 ion from reaction of *m/z* 47 ions on two DEMP molecules.

3.3. Ion/molecule reactions induced by negative alkoxide species

As previously shown [3,31], in a conventional ion trap (i.e. under in situ electron capture ionization conditions) both positive and negative species are trapped concurrently. However, formation efficiency of negative ions is very low compared to the formation of positive ions and hence the proportion of negative species is weak. It is quite difficult to invert the positive/negative ion ratio during these in situ ionization conditions. An interesting alternative is to form negative ions outside the ion trap and then inject them into the ion trap cell. The homemade Q/ITMS tandem offers an attractive possibility to study the reactivity of selected negative ions such as the RO^- alkoxides toward the acid and/or electrophilic DEMP reagent.

Instead of introducing directly the RO^- alkoxide into the ion-trap cell, the corresponding proton-bound homogeneous $[RO^-]_2H^+$ dimers were selectively introduced. Selection of the dimeric ions was preferred

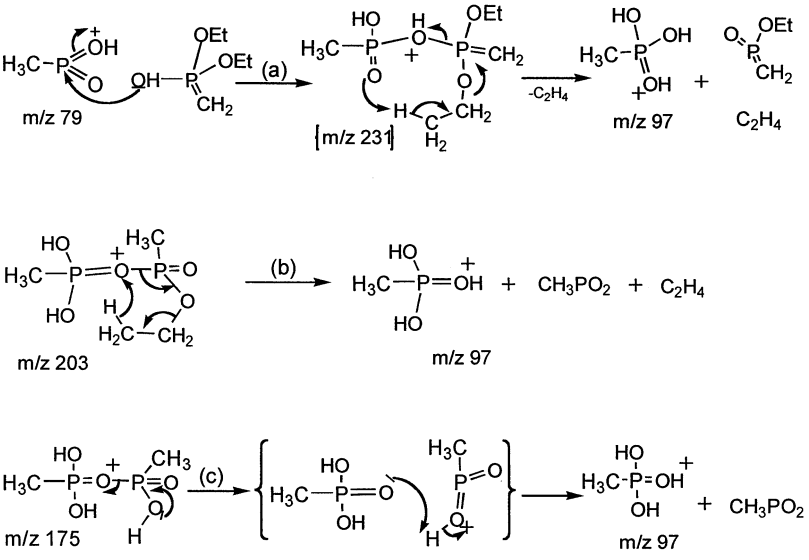

Scheme 5. Formation of *m/z* 97 ions through ion/molecule reactions; (a) from the decomposition of the [DEMP, $H_3C–P(O)_2H^+$] *m/z* 231 adduct ion; (b) from the decomposition of the *m/z* 203 ion; (c) from the *m/z* 175 ion via an isomerization into an ion–dipole complex.

Table 2
Product ions observed during ion/molecule reactions between selected alkoxide reagent and DEMP neutrals after a reaction time of 50 ms, the ΔH^0_{acid} of the alcohols are also reported

Alkoxide reagent	Product ions						ΔH^0_{acid} [35] kJ mol^{-1}
CH_3O^-	*m/z* 31 (31)		*m/z* 123 (5)	*m/z* 151 (64)			1595
$CH_3CH_2O^-$	*m/z* 45 (1)		*m/z* 123 (7)	*m/z* 151 (88)			1582
$(CH_3)_2CHO^-$	*m/z* 58 (6)		*m/z* 123 (38)	*m/z* 151 (50)	*m/z* 165 (2)		1572
$CH_3(CH_2)_3O^-$	*m/z* 73 (11)		*m/z* 123 (1)	*m/z* 151 (88)			1570
$(CH_3)_3CO^-$	*m/z* 73 (2)	*m/z* 57 (11)	*m/z* 123 (7)	*m/z* 147 (1)	*m/z* 151 (71)	*m/z* 275 (0.5) *m/z* 351 (0.5)	1566

to that of the corresponding RO^- monomers because the former is characterized by a lower ΔH^0_f value. Consequently, the injected dimer ions allow the in situ production of the RO^- monomeric anion with a very weak internal energy.

Thus, the injected proton-bound $[RO^-]_2H^+$ dimer dissociates in the ion trap reaction cell into the alkoxide RO^- reagent possessing a weak internal energy. During the injection step, the dimer decomposition yields relaxed alkoxides able to react with DEMP molecules (ΔH^0_{acid} close to 1500 kJ mol^{-1} for alkylphosphonate [29]) which are more acidic than the alcohols (ΔH^0_{acid} higher than 1550 kJ mol^{-1} [32–35]). Table 2 summarizes the product ions generated by the ion/molecule reactions induced by various alkoxides characterized by various ΔH^0_{acid}. The acidity parameter has been chosen in order to investigate the influence of the alcohol acidity on the proton transfer process [33] via formation of an adduct ion [Eq. (3)] and the influence of the reagent ion structure on the reaction orientation relative to other processes such as nucleophilic substitution (Scheme 6) and/or α–β elimination [34] (Scheme 6)

$$[RO^-]_2H^+ \xrightarrow[(-ROH)]{} RO^- \xrightarrow{+DEMP} [DEMP, RO^-] \longrightarrow [DEMP - H]^- + ROH \quad (3)$$

In these experiments, the deprotonated [DEMP − H]$^-$ (*m/z* 151) molecule is produced by the exothermic proton transfer from DEMP to the RO^- alkoxide. Because the exothermicity is carried out by the produced neutral, formation of the [(DEMP − H) − C_2H_4]$^-$ (*m/z* 123) ion cannot be attributed to the dissociation of [DEMP − H]$^-$ (*m/z* 151) but can be generated via ion/molecule reactions.

3.3.1. Reaction with isopropyl alkoxide $(CH_3)_2CHO^-$ (m/z 59): S_N2–C and S_N2–P processes

Fig. 5 shows the dependence of the relative abundance of the *m/z* 59 reagent ions and the produced ions upon the reaction time. Among the various reactions observed, the exothermic proton transfer from DEMP to the nucleophilic reagent RO^- alkoxide appears to be more strongly favored than the other competitive processes, as expected, because of the exothermic nature of the reaction. This yields the formation of the deprotonated [DEMP − H]$^-$ molecule (*m/z* 151) that increases with the reaction time.

Minor pathways involving the formation of both *m/z* 123 and *m/z* 165 ions are observed even at long reaction times. This suggests that these species are also generated by a bimolecular process rather than by a dissociation pathway (Scheme 2). The *m/z* 123 ion may be generated by an α–β elimination mechanism [34] and/or by a S_N2–C as shown in Scheme 6.

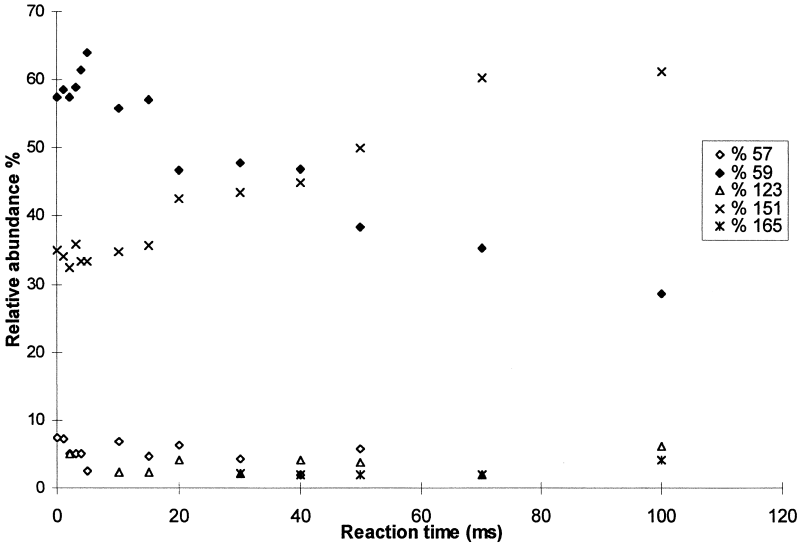

Fig. 5. Evolution (in relative abundance) of the ion/molecule reactions occurring between isopropyl-alkoxide *m/z* 59 and DEMP with the reaction time (ms) yielding *m/z* 123, *m/z* 151, and *m/z* 165.

However, from other investigations, it is evident that the elimination process plays a minor role because the equivalent ions observed during the nucleophilic attack of alkoxides on deprotonated dimethylmethylphosphonate cannot undergo α–β elimination [33d–e]. Thus, the *m/z* 123 ion must be generated via a S_N2–C process rather than the C_2H_4 elimination. Very likely, an intrinsic barrier must be present in the S_N2–C energy diagram, which hinders the reaction. The tight transition state rationalizes the low efficiency of the reaction.

On the other hand, the $[(DEMP - H - C_2H_5O) + C_3H_7O]^-$ *m/z* 165 ion is produced via a S_N2–P process [33d, e] by direct nucleophilic attack at the phosphorous atom induced by the alkoxide reagent leading to an EtO^-/$iProO^-$ exchange. This takes place via the formation of: (1) either a pentavalent intermediate transition state [33d] (i) from which the negative charge reversibly promotes the P–OEt bond cleavage (Scheme 7) or; (2) a direct displacement of the transition state [33d] via a noncovalent S_N2–P transition state (ii) that evolves toward the P–OEt bond cleavage (Scheme 7). Very likely, the evolution of the (i) or (ii) intermediate toward the loss of EtO^- during

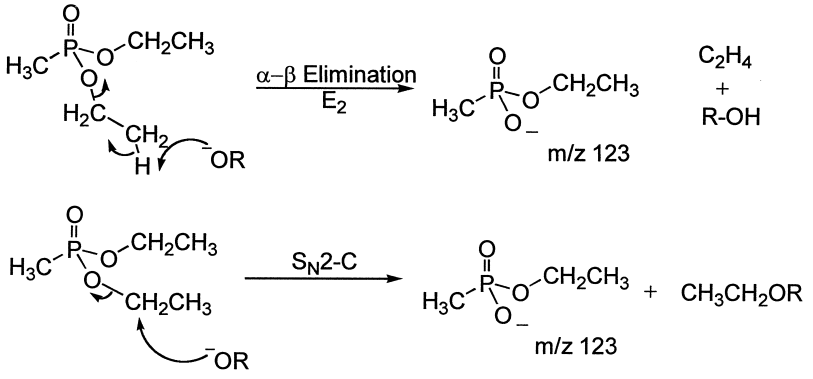

Scheme 6. α–β Elimination or S_N2–C processes occurring during the reaction induced by an alkoxide reagent.

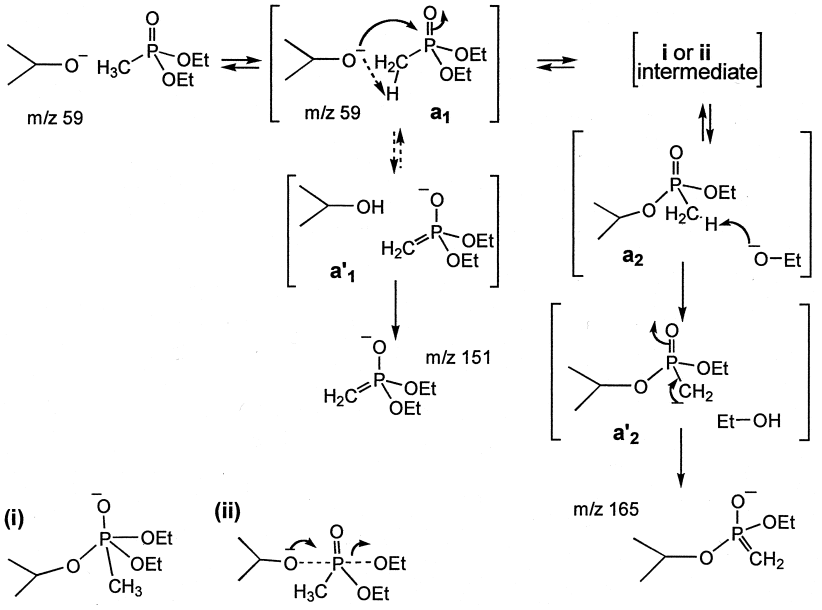

Scheme 7. Formation of the *m/z* 165 ions by $EtO^-/iPrO^-$ exchange process via a pentavalent intermediate transition state **i** or a S_N2–P transition state **ii** leading to a common ion–dipole complex.

the ion–dipole complex formation is probably more endothermic than the reaction pathway leading to the loss of $iPrO^-$. This can explain the decreased efficiency of the reaction yielding *m/z* 165 compared to the formation of *m/z* 151. However, from the assumed ion–dipole complex the internal proton transfer from the PCH_3 group to free ethoxide component takes place through an exothermic ion–dipole isomerization pathway ($a_2 \leftrightarrow a_2'$). This is more exothermic than the isomerization ($a_1 \leftrightarrow a_1'$) implying the alternative ion dipole [iPrOH, $O{=}P(OEt)_2CH_2^-$] (i.e. a_1) because of the following acidity order: $\Delta H^0_{acid}(EtOH) > \Delta H^0_{acid}(iPrOH)$[35] $> \Delta H^0_{acid}(O{=}P(OEt)_2CH_3)$ that shows that ethanol is less acidic than other neutrals. This is based upon the assumption that the acidity of methylphosphonate is higher (or close) to that of the alkylacetate. Finally, such a multistep process (Scheme 7) prior to dissociation probably implies an intrinsic energy barrier that limits the efficiency of the ion–dipole complex yielding the *m/z* 165 diagnostic ion. Such a process has also been observed by Mathurin et al. [7c] from similar substrates using a modified ion trap coupled with a high pressure external source [7].

3.3.2. Reaction products with tertiobutyl-alkoxide (m/z 73)

In spite of the relatively high acidity of tertiary butyl alcohol, deprotonation remains the major process (Fig. 6) contributing to more than 60% of total ionic current. As the reaction time increases, the *m/z* 151 parent ion is almost constant and slightly increases. Alternatively, whatever the origin of the $[DEMP - H - C_2H_4]^-$ (*m/z* 123) ion is (Scheme 6), its abundance is low but increases with the reaction time, reflecting its bimolecular origin.

Note that the competitive S_N2–P pathway is entirely hindered because the $[(DEMP + tC_4H_9O) - C_2H_5OH]^-$ (*m/z* 179) ion is not observed. This suggests that the previously envisaged intrinsic barrier accompanying the S_N2–P pathway has increased because of the tButO$^-$ alkoxide. Indeed, this nucleophilic reagent must lead to a larger steric hindrance during the transition state that lowers the efficiency of this ion/molecule reaction. It can be noticed that the produced *m/z* 123 ion reacts by electrophilic attachment with the DEMP neutral to form the adduct *m/z* 275 ion (~2% of the total ionic current). These hydrogen-bound heterodimers may be stable enough

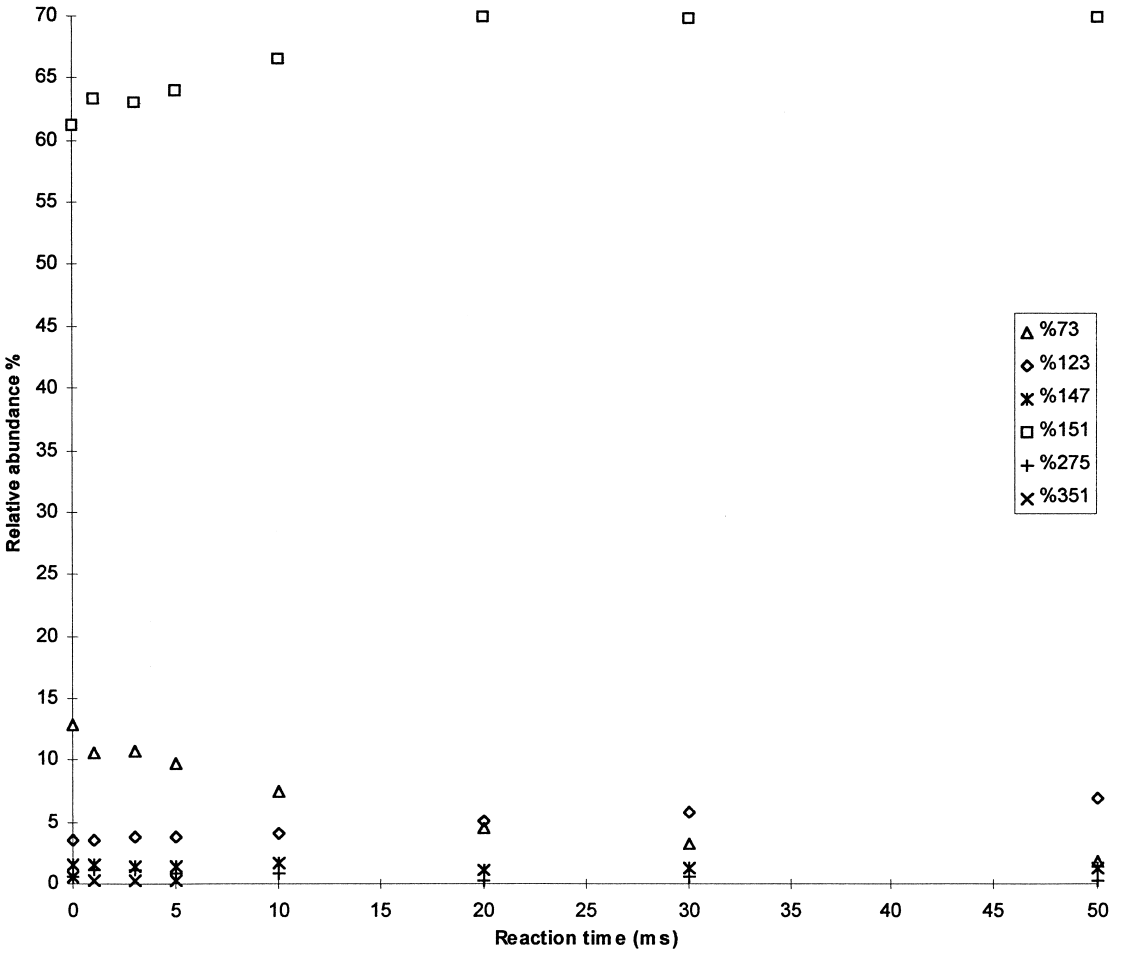

Fig. 6. Evolution in relative abundance of the ion/molecule reaction between tertiobutyl-alkoxide *m/z* 73 and DEMP with the reaction time yielding *m/z* 123, *m/z* 141, *m/z* 151, *m/z* 275, and *m/z* 351.

and the acidity value of each component of dimer should be relatively close. Other adduct ions such as *m/z* 351 are formed but their mechanisms of formation remain unknown and investigations are in progress to explain their formation. A cluster $[(DEMP)_2 + PO]^-$ ion could be a possible candidate to explain formation of the *m/z* 351 ions.

4. Conclusion

Investigation of the injection of the selected $DEMPH^+$ ions prepared and relaxed in the EI/CI external source of our homemade orthogonal tandem quadrupole/ion trap instrument shows that the injection rf level influences the efficiency of the stable long life ion trapping. The mass spectra recorded using the conventional analytical scan displays the injected parent MH^+ and $[M - H]^-$ ions as a base peak only through a narrow LMCO range. The LMCO increase enhances competitive and consecutive parent ion dissociations observed in ERMS experiments recorded using a triple quadrupole instrument.

The advantage of the tandem is the user's ability to study specific ion/molecule reactions. It is possible to select and inject FH^+ fragment ions of DEMP; after a period of isolation the ions can react with the DEMP

neutral directly introduced in the ion-trap reaction cell. The observed processes mostly involved the exothermic proton transfers yielding a protonated $DEMPH^+$ molecule and a proton-bound $DEMP_2H^+$ homodimer that are generated by consecutive thermal collision with a DEMP neutral. It must be emphasized that from the *m/z* 125 and *m/z* 137 reagent ions, the proton-bound [FH^+, DEMP] heterodimer is sufficiently stable to be detected. This is because of the close gas phase basicity between both the neutrals constituting this hydrogen-bound dimer. But this is not the case with the *m/z* 65, *m/z* 97, *m/z* 109, and *m/z* 123 reagent ions leading only to a protonated monomer and homodimer. Reversibly, the other reagent ions such as *m/z* 47, *m/z* 79, *m/z* 81, *m/z* 91, *m/z* 93, and *m/z* 107 (characterized by corresponding neutrals having very weak basicities relative to DEMP) undergo other reactive pathways and highly efficient proton transfer to a DEMP neutral. Reaction of the last group of ions produces reactive pentavalent adduct ions by electrophilic attack at the phosphorous atom rather than forming hydrogen-bound heterodimers by proton chelation. The charge at the oxygen atom promotes neutral loss with a high rate constant because the corresponding precursor covalent adduct ions are not detected, except in the reaction when *m/z* 91 was used as the reagent ion.

Investigation of the behavior of negative ions with the DEMP in the ion trap reaction cell has been very informative. Indeed, negative ions were prepared, in the external NICI source, from different alcohols (as stable even-electron species). Specific bimolecular reactions have been observed because neutral alcohols cannot enter into the ion trap cell and cannot interfere with DEMP neutrals. The main process observed with the alkoxide nucleophilic reagent is DEMP deprotonation. Furthermore, other competitive processes take place. In particular, the S_N2–P process yields the formation of an ion–dipole complex that is able to isomerize by internal proton transfer (according to the component relative acidities) and dissociates into specific species. It appears that this process is sensitive to the steric hindrance when tertiary alcohols are used. A kinetic approach of this reaction has been performed, however, at the limit of sensitivity it was difficult to investigate the temperature effect on the bimolecular rate constants to prove the existence of an eventual intrinsic barrier. In the future, a pulsed counter electrode will be introduced in back of the end electrode related to detection [36], to improve the ion trapping step efficiency. This improvement will permit the study of more subtle effects such as the stereochemical effect of the S_N2–C and S_N2–P processes on diastereoisomeric phosphonates.

References

[1] S. Schachterle, R.D. Brittain, J.D. Mills, J. Chromatogr. A 683 (1994) 185.
[2] V. Drevenkar, B. Stengl, Z. Frobe, Anal. Chem. Acta 290 (1994) 277.
[3] S. Catinella, P. Traldi, X. Jiang, F.A. Londry, R.J.S. Morrison, R.E. March, S. Gregoire, J.-C. Mathurin, J.-C. Tabet, Rapid Commun. Mass Spectrom. 9 (1995) 1302.
[4] J.-C. Mathurin, S. Gregoire, A. Brunot, J.-C. Tabet, R.E. March, S. Catinella, P. Traldi, J. Mass Spectrom. 32 (1997) 829.
[5] (a) N. Mechin, J. Plomley, R.E. March, T. Blasco, J.C. Tabet, Rapid Commun. Mass Spectrom. 9 (1995) 5; (b) N. Mechin, Thesis, Université Pierre et Marie Curie Paris VI, 1997.
[6] S.A. McLuckey, G.J. Van Berkel, D.E. Goeringer, G.L. Glish, Anal. Chem. 66 (1994) 689.
[7] J.-C. Mathurin, S. Grégoire, A. Brunot, J.-C. Tabet, Proceedings of the 45th Conference on Mass Spectrometry and Allied Topics, Palm Spring, CA, 1997, p. 149; (b) T. Faye, J.-C. Mathurin, A. Brunot, C. Fuché, J.-C. Tabet, Proceedings of the 46th Conference on Mass Spectrometry and Allied Topics, Orlando, FL, May 1998, p. 481; (c) J.-C. Mathurin, Thesis, Université Pierre et Marie Curie Paris VI, 1997; (d) T. Faye, J.-C. Mathurin, A. Brunot, J.C. Tabet, G. Wells, C. Fuché, unpublished.
[8] J.C. Schwartz, R.E. Kaiser Jr., R.G. Cooks, P.J. Savickas, Int. J. Mass Spectrom. Ion Processes 98 (1990) 209.
[9] M.J.-F. Suter, H. Gfeller, U.P. Schlunegger, Rapid Commun. Mass Spectrom. 3 (1989) 62.
[10] P. Kofel, H. Reinhard, U.P. Schlunegger, Org. Mass Spectrom. 26 (1991) 463.
[11] R.E. Pedder, R.A. Yost, Proceedings of the 37th Conference on Mass Spectrometry and Allied Topics, Miami Beach, FL, May 1989, p. 468.
[12] G.C. Stafford Jr., P.E. Kelley, J.E.P. Syka, W.E. Reynolds, J.F.J. Todd, Int. J. Mass Spectrom. Ion Processes 60 (1984) 85.
[13] J.E.P. Syka, J.N. Louris, P.E. Kelley, G.C. Stafford, W.E. Reynolds, U.S. Patent 4736101, 1988.
[14] (a) M. Mesilaakso, E.-L. Tolppa, Anal. Chem. 68 (1996)

2313; (b) A.J. Bell, D. Despeyroux, J. Murrell, P. Watts, Int. J. Mass Spectrom Ion Processes 165/166 (1997) 533.
[15] (a) J.S. Brodbelt, H.I. Kenttämaa, R.G. Cooks, Org. Mass Spectrom. 23 (1988) 6; (b) J.R. Holtzclaw, J.R. Wyatt, Org. Mass Spectrom. 23 (1988) 261; (c) L. Zeller, J. Farrel Jr., P. Vainiotalo, H.I. Kenttämaa, J. Am. Chem. Soc. 114 (1992) 1205.
[16] J.R. Holtzclaw, J.R. Wyatt, J.E. Campana, Org. Mass Spectrom. 20 (1985) 90.
[17] (a) A.P. Snyder, C.S. Harden, Org. Mass Spectrom. 25 (1990) 53; (b) S.-A. Fredriksson, L.-G. Hammarström, L. Henriksson, H.-A. Lakso, J. Mass Spectrom. 30 (1995) 1133.
[18] P. Kofel, R.E. March, J.F.J. Todd (Eds.), Practical Aspects of Ion Trap Mass Spectrometry, CRC, Boca Raton, FL, 1995, p. 51.
[19] (a) D.B. Robb, M.W. Blades, Rapid Commun. Mass Spectrom. 13 (1999) 1079; (b) V. Steiner, C. Beaugrand, P. Liere, J.-C. Tabet, J. Mass Spectrom. 34 (1999) 511.
[20] K.L. Busch, G.L. Glish, S.A. McLuckey, Mass Spectrometry Techniques and Applications of Tandem Mass Spectrometry, VCH, New York, 1988, p. 78.
[21] M. Wensing, A.P. Snyder, C.S. Harden, J. Mass Spectrom. 30 (1995) 1539.
[22] M. Wensing, A.P. Snyder, C.S. Harden, Rapid Commun. Mass Spectrom. 10 (1996) 1259.
[23] F.G. Major, H.G. Dehmelt, Phys. Rev. 170 (1968) 91.
[24] C.S. Harden, A.P. Snyder, G.A. Eiceman, Org. Mass Spectrom. 28 (1993) 585.
[25] A.G. Harrison, in Chemical Ionization Mass Spectrometry, 2nd edn., CRC, Boca Raton, FL, 1992, p. 95.
[26] (a) S.A. McLuckey, D. Cameron, R.G. Cooks, J. Am. Chem. Soc. 103 (1981) 6; (b) R. Orlando, C. Fenselau, R.J. Cotter, J. Am. Chem. Soc. 112 (1990) 5747.
[27] (a) A. Ranasinghe, R.G. Cooks, S.K. Sethi, Org. Mass Spectrom. 27 (1992) 77; (b) M. Meot-Ner, J. Am. Chem. Soc. 114 (1992) 3312.
[28] M. Meot-Ner, J. Am. Chem. Soc. 106 (1984) 1257.
[29] (a) A. Leroy, F. Fournier, J.-C. Tabet, J. Dissard, I. Daoust-Maleval, A. Tambuté, Proceedings of the 43rd Conference on Mass Spectrometry and Allied Topics, Atlanta, GA, May 1995, p. 406; (b) A. Leroy, Thesis, Université Pierre et Marie Curie Paris VI, 1996.
[30] (a) P. Liere, T. Blasco, R.E. March, J.C. Tabet, Rapid Commun. Mass Spectrom. 8 (1994) 953; (b) P. Liere, S. Bouchonnet, R.E. March, J.-C. Tabet, Rapid Commun. Mass Spectrom. 9 (1995) 1594.
[31] D.W. Berberich, R.A. Yost, J. Am. Soc. Mass Spectrom. 5 (1994) 757.
[32] S.G. Lias, J.E. Bartmess, J.F. Liebman, J.L. Holmes, R.D. Levin, W.G. Mallard, Gas phase ion and neutral thermochemistry, J. Phys. Chem. Ref. Data 17 (1988) (suppl.).
[33] (a) R.V. Hodges, S.A. Sullivan, J.L. Beauchamp, J. Am. Chem. Soc. 102 (1980) 935; (b) E.S. Lightcap, P.A. Frey, J. Am. Chem. Soc. 114 (1992) 9750; (c) A.C. Hengge, W.A. Edens, H. Elsing, J. Am. Chem. Soc. 116 (1994) 5045; (d) R.C. Lum, J.J. Grabowski, J. Am. Chem. Soc. 114 (1992) 8619; (e) R.C. Lum, J.J. Grabowski, J. Am. Chem. Soc. 115 (1993) 7823.
[34] (a) L.J. De Koning, N.M.M. Nibbering, J. Am. Chem. Soc. 110 (1988) 2066; (b) G. Occhiucci, M. Speranza, L.J. De Koning, N.M.M. Nibbering, J. Am. Chem. Soc. 111 (1989) 7387.
[35] M.J. Haas, A.G. Harrison, Int. J. Mass Spectrom. Ion Processes 124 (1993) 115.
[36] A. Mordehai, Proceedings of the 45th ASMS Conference on Mass Spectrometry and Allied Topics, Palm Springs, CA, June 1997, p. 128.